NANO MICRO small

Nebulized Gadolinium-Based Nanoparticles: A Theranostic Approach for Lung Tumor Imaging and Radiosensitization

*Sandrine Dufort, Andrea Bianchi, Maxime Henry, François Lux, Géraldine Le Duc, Véronique Josserand, Cédric Louis, Pascal Perriat, Yannick Crémillieux, Olivier Tillement, and Jean-Luc Coll**

Lung cancer is the most common and most fatal cancer worldwide. Thus, improving early diagnosis and therapy is necessary. Previously, gadolinium-based ultra-small rigid platforms (USRPs) were developed to serve as multimodal imaging probes and as radiosensitizing agents. In addition, it was demonstrated that USRPs can be detected in the lungs using ultrashort echo-time magnetic resonance imaging (UTE-MRI) and fluorescence imaging after intrapulmonary administration in healthy animals. The goal of the present study is to evaluate their theranostic properties in mice with bioluminescent orthotopic lung cancer, after intrapulmonary nebulization or conventional intravenous administration. It is found that lung tumors can be detected non-invasively using fluorescence tomography or UTE-MRI after nebulization of USRPs, and this is confirmed by histological analysis of the lung sections. The deposition of USRPs around the tumor nodules is sufficient to generate a radiosensitizing effect when the mice are subjected to a single dose of 10 Gy conventional radiation one day after inhalation (mean survival time of 112 days versus 77 days for irradiated mice without USRPs treatment). No apparent systemic toxicity or induction of inflammation is observed. These results demonstrate the theranostic properties of USRPs for the multimodal detection of lung tumors and improved radiotherapy after nebulization.

Dr. S. Dufort, M. Henry, Dr. V. Josserand, Dr. J.-L. Coll
INSERM U823
Institut Albert Bonniot
38706, Grenoble cedex, France
E-mail: Jean-luc.coll@ujf-grenoble.fr

Dr. S. Dufort, M. Henry, Dr. V. Josserand, Dr. J.-L. Coll
Université Joseph Fourier
Institut Albert Bonniot
38706, Grenoble cedex, France

Dr. S. Dufort, Dr. C. Louis
Nano-H S.A.S.
2 place de l'Europe 38070, Saint Quentin – Fallavier, France

Dr. A. Bianchi, Dr. Y. Crémillieux
Centre de Résonance Magnétique des Systèmes Biologiques
UMR 5536 CNRS
Université Bordeaux Segalen
146 rue Léo Saignat 33076, Bordeaux, France

Dr. F. Lux, Prof. O. Tillement
Institut Lumière Matière
UMR 5306 CNRS, Université Lyon 1-CNRS
Université de Lyon
69622, Villeurbanne cedex, France

Dr. G. Le Duc
Biomedical Beamline
European Synchrotron Radiation Facility
6 rue Jules Horowitz
38043, Grenoble cedex, France

Prof. P. Perriat
Matériaux Ingénierie et Science
INSA Lyon, UMR 5510 CNRS
Université de Lyon
69621, Villeurbanne cedex, France

DOI: 10.1002/smll.201401284

1. Introduction

Lung cancer (including both non-small cell lung cancer (NSCLC) and small cell lung cancer (SCLC)) is a major health problem and is the leading cause of cancer-related adult deaths worldwide.[1] Despite current technological and medical advances, the majority of patients are diagnosed with locally advanced or metastatic disease, that is in operable in most cases.[1,2] In these instances, concomitant chemo-radiation therapy remains the most effective therapy[3] but the 5-year survival rate is only 15%.[4]

The reasons for therapeutic failure are diverse and are partially due to the inability to achieve adequate concentrations of drugs at the tumor site after systemic administration.[5] To increase exposure of the tumor to therapeutic agents while minimizing systemic side-effects, regional chemotherapy is a promising method and has already been successfully applied for the treatment of ovarian,[6] brain[7] and bladder tumors[8] and liver metastasis.[9]

Inhalation of anti-tumor agents may be an alternative administration route to improve lung cancer outcomes. Indeed, the lungs present a large surface area for drug absorption and an extensive vasculature with a weak anatomical barrier that does not limit access to the body.[10,11] The first trial, performed by Shevchanko and Resnik in 1968, established the feasibility and the efficacy of administering chemotherapy by inhalation in combination with radiotherapy.[12] Since then, a large number of drugs have been investigated for intrapulmonary administration in animal models and in human trials.[11,13–15] In recent years, the pulmonary administration of nanoparticles has become an attractive strategy for the local delivery of therapeutic or diagnostic compounds[16]; however, to the best of our knowledge, only one work discusses the pulmonary administration of iodinated nanoparticles for diagnostic purposes.[17] With the exception of Pulmozyme, a recombinant human DNase, the airways are mainly used for small drug delivery because it is reducing significantly the passage of larger molecules such as antibodies to the bloodstream (the hydroscopic diameter of an antibody is 10 to 20 nm). It is thus important to study the behavior of ultrasmall nanoparticles display hydrodynamic diameters <6 nm to understand better their properties in this context. Since the amount and location of nanoparticles deposition will vary with ventilation parameters such as the inspiratory flow rate and forced expiratory volume, patients suffering with airway obstruction may not be eligible to aerosoltherapies. On the other hand, patients with lepidic non small cell lung cancers, with secondary lung metastasis, or with diffuse idiopathic pulmonary neuroendocrine cell hyperplasia (DIPNECH) or patients for whom it is important to vary the treatments may really benefit from aerosoltherapies.

Radiotherapeutic failure can be attributed to the resistance of tumors located in the lung, a highly radio-sensitive organ. This intrinsic property of the lung prevents the use of elevated doses of radiation during radiotherapy because of the resulting major side effects. The local deposition of nanoparticles containing high Z-elements, such as gold, platinum or gadolinium, on the tumor site could enhance the effects of X-rays.[18–21] This should maximize the radiotherapeutic efficacy via the increase of toxicity on the tumor tissues and result in only minor side effects in normal tissues.

In this context, we developed "theranostic" ultra-small rigid particles, USRPs, obtained via an original top-down process. These particles are composed of a polysiloxane matrix and chelating species, e.g., DOTA (1,4,7,10-tetraazacyclododecane-1,4,7,10-tetraacetic acid), which is covalently grafted on the inorganic surface. In previous studies, the particles were validated as promising multimodal contrast agents for complementary imaging techniques, i.e., magnetic resonance imaging (MRI), single-photon emission computed tomography (SPECT), computed tomography (CT) and fluorescence imaging.[22] Despite rapid blood and renal clearance due to their small size (<6 nm),[23] the significant accumulation of these multifunctional particles in tumors occurs after intravenous injection, as a result of a passive targeting mechanism related to the enhanced permeability and retention (EPR) effect[24] and of a specific active tumor-targeting mechanism after the grafting of cRGD peptides on their surface as demonstrated in a former study.[25] Finally, these gadolinium-based nanoparticles exhibited high radiosensitizing properties in vitro and in vivo.[21,26]

In a recent study, the biodistribution and pharmacokinetics of USRPs were investigated by ultrashort echo-time MRI (UTE-MRI) and fluorescence imaging after intrapulmonary administration in healthy mice.[27] The two imaging techniques showed similar kinetics for USRPs, with the occurrence of renal clearance after rapid passage from the airways to the bloodstream (elimination time of 187 ± 40 min).

We undertook the present study to evaluate deep lung tumor detection by fluorescence imaging and MRI in vivo and the radiosensitizing effect of USRPs administered directly in the airways of mice bearing orthotopic human lung tumors (H358-Luc). We also evaluated the potential inflammation induced by intrapulmonary administration of the nanoparticles in a NF-κB-RE-Luc transgenic mouse model.

2. Results and Discussion

2.1. In Vivo Lung Tumor Detection

An orthotopic mouse model of human NSCLC was developed. Orthotopic models take into account the microenvironment of tumors. Thus, they are more relevant than the widely used subcutaneous xenografts to evaluate the diagnostic and/or therapeutic properties of novel agents.[29] In this model, lung tumors develop after the intrapulmonary inoculation of luciferase-modified human NSCLC H358 cells (H358-Luc cells). The use of bioluminescence in vivo is convenient for the non-invasive monitoring of the implantation and growth of these orthotopic tumors over five weeks.[30] At this time point, tumors are well-developed with a strong bioluminescent signal, but this is before the appearance of obvious symptoms (e.g., body weight loss and breathing difficulties). Mice bearing H358-Luc lung tumors can thus be used for subsequent imaging and/or therapy studies before the lung

DOI: 10.1002/smll.201401284

NANO MICRO small

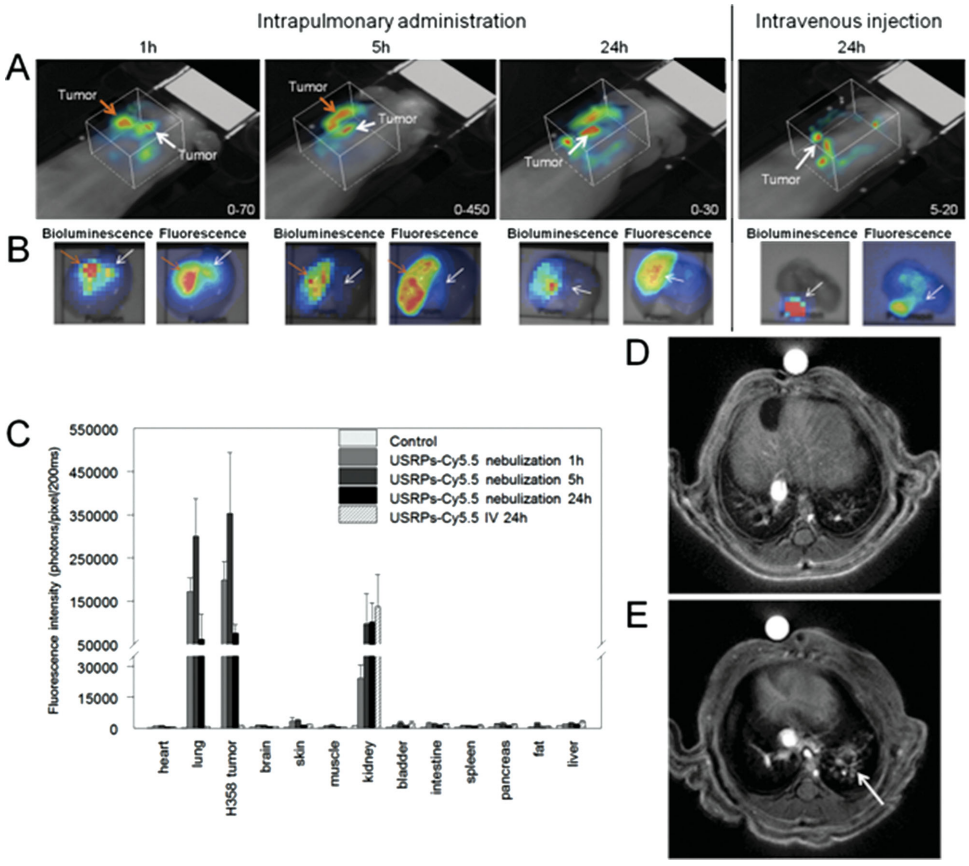

Figure 1. In vivo H358-Luc orthotopic lung tumor imaging. (A) In vivo fluorescence tomography imaging after intrapulmonary or intravenous injection of USRPs-Cy5.5 (50 µL at [Gd^{3+}] ~40 mM, n = 3). (B) Bioluminescence and fluorescence imaging were then performed on isolated lungs, and showed a colocalization between the H358-Luc tumors (bioluminescence) and the fluorescent nanoparticles (fluorescence) (arrows). (C) Biodistribution of the fluorescent nanoparticles at different time points after intrapulmonary administration or 24 h after intravenous injection, was evaluated by defining ROIs on fluorescent images of extracted organs. (D,E) USRPs also permitted the detection of lung tumors by MRI as can be seen before (D) or after (E) intrapulmonary instillation (50 µL at [Gd^{3+}] ~50 mM).

tumors induce breathing distress that could interfere with their health.

The ability of USRPs labeled with Cyanine 5.5 (USRPs-Cy5.5) to improve the in vivo detection of lung tumors was first evaluated after intrapulmonary or intravenous administration of equal quantities of nanoparticles using 3D-fluorescence tomography imaging. This was performed at multiple time points after intrapulmonary administration of 50 µL of a solution containing ~40 mmol/L [Gd^{3+}] or after intravenous injection of 200 µL of ~10 mmol/L [Gd^{3+}]. Representative images are shown in **Figure 1**A.

At the end of the experiment, the mice were euthanized, and the extracted organs were subjected to ex vivo bioluminescence and fluorescence imaging (Figure 1B) for semi-quantification (Figure 1C). In both cases, in vivo and ex vivo, bioluminescence or fluorescence imaging showed similar profiles. USRPs-Cy5.5 were homogeneously distributed into the lungs immediately after intrapulmonary administration. Highly fluorescent spots could be observed on both the 3D-fluorescence images and ex vivo fluorescence images of the lungs. These high-intensity zones corresponded to the tumor nodules, as established by bioluminescence imaging (arrows on Figure 1A and B). This was associated with the augmented, but not significantly different, uptake of USRPs-Cy5.5 in lungs bearing tumors compared to "normal" lungs. Regarding intravenous injection, USRPs-Cy5.5 were barely detectable in the tumor, with an augmented signal two times that of the normal lungs (P = 0.0209). Nonetheless, at 24 h, the fluorescent signal was 52 times lower in the tumors when the particles were injected intravenously compared to intrapulmonary administration of the same quantity of injected nanoparticles. Interestingly, the two different administration routes resulted in similar levels of non-specific accumulation of the fluorescent USRPs in all of the other organs assessed (especially in the spleen and in the liver) with a similar mode of elimination via the kidneys, thus showing agreement with our previous data.[22,27] These results confirmed that direct administration via the airways can increase the amount of locally delivered molecules or nanoparticles in lung tumor models, which could be of great interest for the treatment of lung diseases.[5,16,31]

Moreover, the intrapulmonary administration of USRPs permitted the detection of lung tumors using the specific UTE-MRI sequence (Figure 1D). This result sustained and validated the multimodal properties of these nanoparticles[21,22,27] and their potential as multimodal contrast agents for the detection of lung tumors.

DOI: 10.1002/smll.201401284

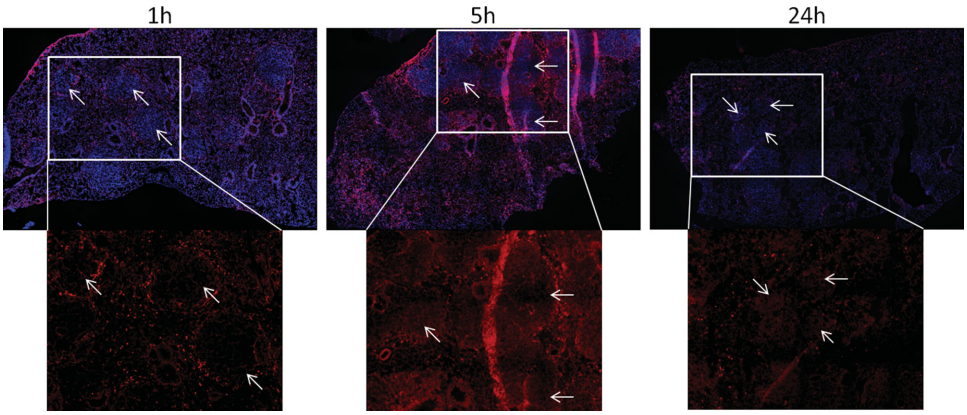

Figure 2. Distribution of fluorescent nanoparticles on the frozen lung sections of H358-Luc tumor-bearing mice at different time points after intrapulmonary administration of USRPs-Cy5.5 (50 µL of ~40 mM [Gd^{3+}]). Lung sections were observed by fluorescence microscopy (in blue: Hoechst staining of the nuclei; in red: Cy5.5 signals). The upper panel presents the superimposed images of the Hoechst and Cy5.5 signals. The bottom panel corresponds to Cy5.5-only signals. The Cy5.5 signal was primarily localized close to the tumor nodules (arrows).

2.2. Lung Distribution of USRPs-Cy5.5 After Intrapulmonary Administration

Fluorescence pseudo-confocal (apotome) microscopy was then performed on frozen lung sections to obtain more precise information about the distribution of USRPs-Cy5.5 within the lung tissues after intrapulmonary administration (**Figure 2**). A large proportion of instilled fluorescent nanoparticles was found in the alveoli 1 h after administration, together with a delineation of the lung tumors. No specific binding of the USRPs to the tumor cells could be detected. The signal was augmented in the periphery of the tumor nodules, suggesting a decreased passage of the nanoparticles to the blood when the tumor are present. Similar patterns were still observable 5 hours and 24 hours after administration, although a decrease of the fluorescent signal in the alveoli was noted. This reduction of the fluorescent signal can most likely be attributed to the passage of the nanoparticles from the airways to the blood, owing to the small size of the nanoparticles (<6 nm),[23] as described in a previous study.[27] A very weak fluorescence signal was detected by fluorescence microscopy on lung sections obtained from mice intravenously injected with USRPs-Cy5.5, in agreement with the 52-times reduction of macroscopic signal. Since we used 9 nm thick sections, this resulted in only a small number of fields of view presenting scattered nanoparticles randomly distributed in the alveoli's (data not shown).

2.3. Radiosensitizing Therapeutic Study

The significant and specific accumulation/retention of USRPs-Cy5.5 around the tumors in the nebulized lungs suggested that a radiosensitizing effect could be expected. H358-Luc lung tumor-bearing mice were therefore exposed to conventional irradiation of 10 Gy after intrapulmonary administration of USRPs (50 µL of ~20 mM [Gd^{3+}]). Prior to treatment, in vivo bioluminescence imaging was performed for all mice, and the bioluminescent signal in the lungs was quantified to randomize the mice into three homogenous groups: (i) a group of mice treated with irradiation after intrapulmonary administration of USRPs (n = 11); (ii) a control group (n = 6; no nanoparticle administration, no irradiation) and (iii) an irradiated-only group (n = 11; no nanoparticle administration, irradiation) (**Figure 3**). The control and irradiated-only mice groups exhibited similar median survival times (MeST) of 83 days and 77 days (no significant difference; $P = 0.926$). In contrast, the MeST was extended to 112 days in the group irradiated in the presence of USRPs. This corresponded to a 45% increase in lifespan (ILS) compared to the irradiated-only group ($P = 0.028$). The improvement was attributed to the radiosensitizing properties of USRPs (containing high-Z gadolinium atoms), which were primarily present at the tumor level during irradiation, as shown by in vivo fluorescence imaging, UTE-MRI, and the analysis of the lung sections. This therapeutic protocol

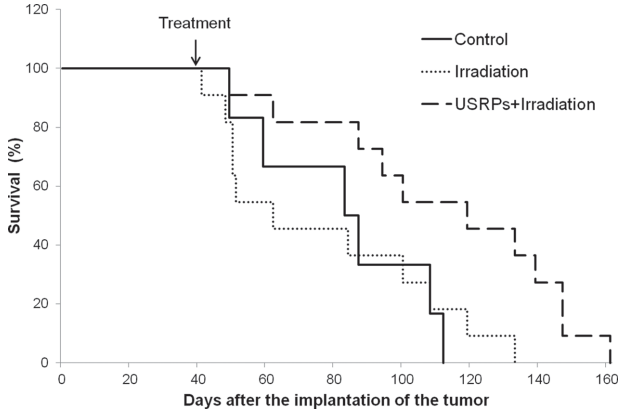

Figure 3. Survival curve comparison obtained on H358-Luc lung tumor-bearing mice without treatment (n = 6), only treated by one irradiation (n = 11), and treated by one irradiation (n = 11) 24 h after the intrapulmonary administration of nanoparticles, 161 days after tumor implantation. The irradiation was performed at 10 Gy, 37 days after tumor implantation.

small 2014,
DOI: 10.1002/smll.201401284

NANO MICRO small

represents an attractive strategy for the treatment of lung tumors in radio-sensitive organs such as the lung.

These results have completed and continued the previous works in which it was initially demonstrated that despite rapid renal elimination after intravenous injection or intrapulmonary administration, USRPs can improve the effect of radiotherapy[21] independent of the location and type of tumor (subcutaneous, brain, etc.).

2.4. Pulmonary Inflammatory Potential of USRPs

Finally, demonstrating the safety of these nanoparticles after intrapulmonary administration was important. In particular, several publications have reported inflammation of the lungs and particle-induced activation of the redox-responsive NF-κB signaling pathway after in vitro exposure[32–34] and after the inhalation or pulmonary delivery[35,36] of nanoparticles. Therefore, the effect of USRPs nebulization in NF-κB-RE-Luc transgenic mice was investigated. We evaluated the potential induction of inflammation that depends on the NF-κB pathway in this strain of transgenic mice, 2, 5, 24, 48, 72 and 96 h after the intrapulmonary administration of USRPs (50 µL of ~20 mM [Gd^{3+}]) (**Figure 4**). Evaluation of the induced inflammation was performed using an ex vivo luciferase enzymatic activity assay on the protein extracts of all representative organs including the lungs, kidneys, spleen, liver and muscle (as a negative control) to generate highly sensitive and quantitative measurements. No significant variation was observed when the luciferase activities in the organs of the treated versus non-treated mice (control) were compared. In contrast, animals that received an intrapulmonary administration of lipopolysaccharide (LPS, 2 mg/kg), which was used as a positive control for lung injury,[37] showed a 8-fold significant increase in luciferase activity in the lungs 24 h after administration compared to the control. These results are also consistent with the broncho-alveolar lavage analyses performed in a previous study[27] that showed no increase in the number of immune cells after intrapulmonary administration of USRPs. This result is not surprising in regard to the chemical composition of USRPs made with very small amount of polysiloxane that crosslink non-inflammatory DOTA-Gd, and in regard to their small size that is associated with a rapid elimination from the lung and the rest of the body.

These results confirmed that the intrapulmonary nebulization of USRPs is a safe and efficient mode of administration of these nanoparticles to the lungs without inducing an inflammatory reaction. These findings corroborate the interest in the intrapulmonary administration modality, which presents several advantages compared to inhalation or intravenous injection for the monitoring of lung tumors.[38–41]

3. Conclusions

This study demonstrates the advantages of using gadolinium-based theranostic nanoparticles (USRPs) in an orthotopic lung cancer mouse model. USRPs enabled the multimodal detection, by fluorescence imaging and MRI, of lung tumors after both intravenous and intrapulmonary administration. Their direct administration into the airways significantly increased their pulmonary delivery and uptake by the tumors, allowing improved detection of the tumor using imaging. In addition, the proposed protocol improved the use of conventional X-ray radiation due to the radiosensitizing properties of USRPs. Moreover, the intrapulmonary administration of nanoparticles did not induce inflammation. Based on these preclinical results, USRPs is anticipated to have potential applications as a simultaneous imaging and therapy modality for selected clinical lung cancer patients in the near future. The next step toward personalized therapy is the use of these nanoparticles for image-guided therapy.

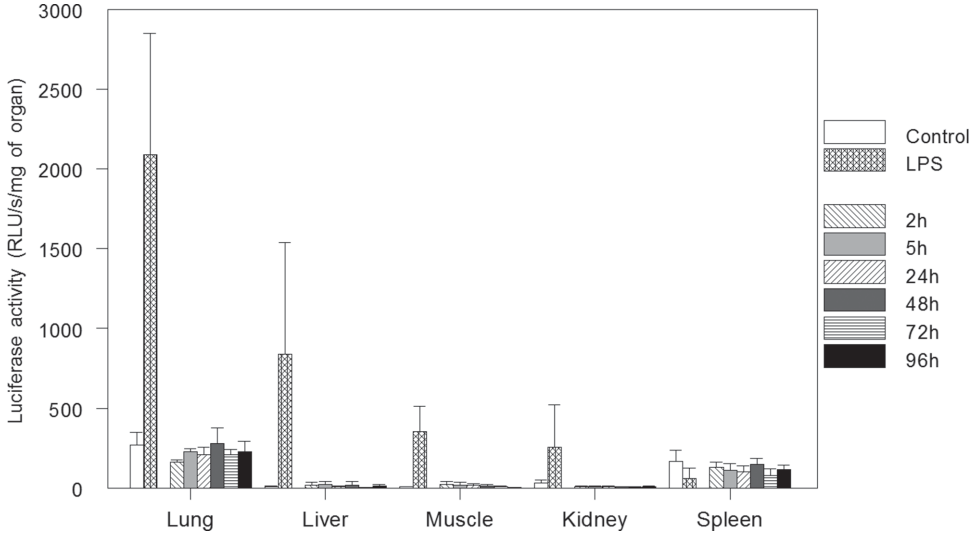

Figure 4. Evaluation of the inflammatory potential of USRPs after intrapulmonary administration. The luciferase enzymatic activity was quantified in organs of NF-κB-RE-Luc mice at different times after the intrapulmonary administration of USRPs (50 µL of ~20 mM [Gd^{3+}]) (n = 5, mean ± SD). As positive control, the mice received an intrapulmonary administration of lipopolysaccharide (LPS, 2 mg/kg) and were sacrificed at 24 h.

DOI: 10.1002/smll.201401284

4. Experimental Section

Nanoparticle Synthesis and Characterization: The Gd-DOTA-based nanoparticles (USRPs) were synthesized and characterized according to the previously described protocol.[22,27,28] To perform the fluorescence imaging, Cyanine 5.5 (Cy5.5) near infrared dye was covalently grafted on the nanoparticles (USRPs-Cy5.5), as described in reference.[25]

Lung Tumor Animal Model: Animal experiments were conducted in accordance with protocols approved by the Ethical Committee of Grenoble. H358-Luc cells (Optimal, Grenoble, France), cultured in RPMI medium supplemented with 10% of heat-inactivated fetal bovine serum, were harvested, washed and resuspended in 1× PBS at 10^7 cells/50 µL. Female NMRI nude mice (6 weeks old) were anesthetized with an intraperitoneal (i.p.) injection of Medetomidin (0.2 µg/g)/Ketamine (0.1 mg/g), and the tumor cells were inoculated in the lungs with a catheter after orotracheal intubation. The monitoring of tumor development was followed by in vivo bioluminescence imaging after the i.p. injection of 150 mg/kg of Luciferin (Promega, Charbonnières, France), as previously described.[42] The quantification of bioluminescent signals allowed for the randomization of animals before each experiment. Lung tumors developed over a period of five weeks.

Intrapulmonary Spray Administration: Intrapulmonary administration was performed using a nebulizing IA-1C Microsprayer (Penn-Century, Inc., PA, USA) connected to a FMJ-250-high-pressure syringe (Penn-Century, Inc.) containing 50 µL of nanoparticles labeled with or without Cy5.5. After i.p. anesthesia with Medetomidin/Ketamine, the tip of the microsprayer was introduced into the trachea of the animals using a dedicated laryngoscope.

Tumor Imaging Study: Bioluminescence, 2D- and 3D-fluorescence imaging, fluorescence quantifications (Optimal, Grenoble, France) and Ultrashort echo-time Magnetic Resonance Imaging (UTE-MRI) were performed as described in previous studies.[27,41,43]

Fluorescence microscopy of the frozen lung sections (9 µm) was carried out using an AxioImager microscope with the AxioVision® software (Carl Zeiss, Jena, Germany) with a 10× objective. Nuclei were labeled by 1 µg/mL of Hoechst 33342 in 1× PBS for 5 min at room temperature.

Therapeutic Efficacy Study: Bioluminescence imaging was performed 35 days after tumor implantation, and animals were randomized into three groups: control (n = 6), irradiation (n = 11) and USRPs + irradiation (n = 11). Irradiation consisted in a single 10 Gy dose delivered with a radiation source operating at 200 keV with a 2 mm Al-filter. Irradiation, restricted to the chest region, was performed at day 37, 24 h after intrapulmonary administration of USRPs (50 µL of ~20 mM [Gd^{3+}]). The mice were followed at the animal facility after irradiation. At a later tumor stage, mice were euthanized when presenting clinical signs and/or 20% weight loss.

Pulmonary Inflammatory Potential of USRPs: At different time points (2, 5, 24, 48, 72, and 96 h) after the intrapulmonary administration of USRPs (50 µL of ~40 mM [Gd^{3+}]), NF-κB-RE-Luc mice (Taconic, USA) were sacrificed (n = 5 for each time point), and the organs were collected and mashed for the in vitro luciferase enzymatic activity assay (Promega, Charbonnières, France), as previously described.[44]

The lipopolysaccharide (LPS) (Sigma-Aldrich, USA) was used as positive control. The mice were sacrificed 24 h after the intrapulmonary administration of LPS (2 mg/kg).

Statistical Analyses: Statistical analyses were performed using the two-tail non-parametric Mann-Whitney t-test. All results are expressed as the mean ± standard deviation. To compare survival among different treatment groups, the Kaplan-Meier survival data were plotted versus time after tumor implantation. These data were subsequently analyzed using a log-rank test. In both cases, statistical significance was considered when $P < 0.05$.

Acknowledgments

The authors acknowledge the funding support of the National Research Agency for the ANR project Gd-Lung (ANR-12-P2N-0009) and of INSERM. In addition, the authors are grateful to the team of the OPTIMAL Grenoble small animal optical imaging facility for their help and technical assistance. A.B. acknowledges a fellowship from the European Network PINET (FP7-PEOPLE-2010-ITN-264864).

[1] A. Jemal, M. J. Thun, L. A. Ries, H. L. Howe, H. K. Weir, M. M. Center, E. Ward, X. C. Wu, C. Eheman, R. Anderson, U. A. Ajani, B. Kohler, B. K. Edwards, *J. Natl. Cancer Inst.* **2008**, *100*, 1672–1694.
[2] D. Morgensztern, S. H. Ng, F. Gao, R. Govindan, *J. Thorac.Oncol.* **2010**, *5*, 29–33.
[3] J. Jassem, *Radiother.Oncol.* **2007**, *83*, 203–213.
[4] K. M. Pisters, W. K. Evans, C. G. Azzoli, M. G. Kris, C. A. Smith, C. E. Desch, M. R. Somerfield, M. C. Brouwers, G. Darling, P. M. Ellis, L. E. Gaspar, H. I. Pass, D. R. Spigel, J. R. Strawn, Y. C. Ung, F. A. Shepherd, *J. Clin. Oncol.* **2007**, *25*, 5506–5518.
[5] F. Gagnadoux, J. Hureaux, L. Vecellio, T. Urban, A. Le Pape, I. Valo, J. Montharu, V. Leblond, M. Boisdron-Celle, S. Lerondel, C. Majoral, P. Diot, J. L. Racineux, E. Lemarie, *J. Aerosol Med. Pulm. Drug Deliv.* **2008**, *21*, 61–70.
[6] W. R. Robinson, C. Coberly, J. Beyer, A. Lewis, C. Ballard, *J. Oncol. Pract.* **2008**, *4*, 225–228.
[7] C. Guerin, A. Olivi, J. D. Weingart, H. C. Lawson, H. Brem, *Invest. New Drugs* **2004**, *22*, 27–37.
[8] M. Wirth, V. E. Plattner, F. Gabor, *Expert Opin. Drug Deliv.* **2009**, *6*, 727–744.
[9] N. E. Kemeny, D. Niedzwiecki, D. R. Hollis, H. J. Lenz, R. S. Warren, M. J. Naughton, J. C. Weeks, E. R. Sigurdson, J. E. Herndon, 2nd, C. Zhang, R. J. Mayer, *J. Clin. Oncol.* **2006**, *24*, 1395–1403.
[10] N. R. Labiris, M. B. Dolovich, *Br. J. Clin. Pharmacol.* **2003**, *56*, 588–599.
[11] P. Zarogoulidis, E. Chatzaki, K. Porpodis, K. Domvri, W. Hohenforst-Schmidt, E. P. Goldberg, N. Karamanos, K. Zarogoulidis, *Int. J. Nanomedicine.* **2012**, *7*, 1551–1572.
[12] A. A. Shvedova, E. Kisin, A. R. Murray, V. J. Johnson, O. Gorelik, S. Arepalli, A. F. Hubbs, R. R. Mercer, P. Keohavong, N. Sussman, J. Jin, J. Yin, S. Stone, B. T. Chen, G. Deye, A. Maynard, V. Castranova, P. A. Baron, V. E. Kagan, *Am. J. Physiol. Lung Cell Mol. Physiol.* **2008**, *295*, L552–565.
[13] J. Hureaux, F. Lagarce, F. Gagnadoux, L. Vecellio, A. Clavreul, E. Roger, M. Kempf, J. L. Racineux, P. Diot, J. P. Benoit, T. Urban, *Eur. J. Pharm. Biopharm.* **2009**, *73*, 239–246.
[14] P. Chao, M. Deshmukh, H. L. Kutscher, D. Gao, S. S. Rajan, P. Hu, D. L. Laskin, S. Stein, P. J. Sinko, *Anticancer Drugs* **2010**, *21*, 65–76.
[15] G. A. Otterson, M. A. Villalona-Calero, W. Hicks, X. Pan, J. A. Ellerton, S. N. Gettinger, J. R. Murren, *Clin. Cancer Res.* **2010**, *16*, 2466–2473.

DOI: 10.1002/smll.201401284

[16] S. Azarmi, W. H. Roa, R. Lobenberg, *Adv. Drug Deliv. Rev.* **2008**, *60*, 863–875.
[17] G. L. McIntire, E. R. Bacon, J. L. Toner, J. B. Cornacoff, P. E. Losco, K. J. Illig, K. J. Nikula, B. A. Muggenburg, L. Ketai, *J. Pharm. Sci.* **1998**, *87*, 1466–1470.
[18] J. F. Hainfeld, F. A. Dilmanian, D. N. Slatkin, H. M. Smilowitz, *J. Pharm. Pharmacol.* **2008**, *60*, 977–985.
[19] M. Y. Chang, A. L. Shiau, Y. H. Chen, C. J. Chang, H. H. Chen, C. L. Wu, *Cancer Sci.* **2008**, *99*, 1479–1484.
[20] E. Porcel, S. Liehn, H. Remita, N. Usami, K. Kobayashi, Y. Furusawa, C. Le Sech, S. Lacombe, *Nanotechnology* **2010**, *21*, 85103.
[21] G. Le Duc, I. Miladi, C. Alric, P. Mowat, E. Brauer-Krisch, A. Bouchet, E. Khalil, C. Billotey, M. Janier, F. Lux, T. Epicier, P. Perriat, S. Roux, O. Tillement, *ACS Nano* **2011**, *5*, 9566–9574.
[22] F. Lux, A. Mignot, P. Mowat, C. Louis, S. Dufort, C. Bernhard, F. Denat, F. Boschetti, C. Brunet, R. Antoine, P. Dugourd, S. Laurent, L. Vander Elst, R. Muller, L. Sancey, V. Josserand, J. L. Coll, V. Stupar, E. Barbier, C. Remy, A. Broisat, C. Ghezzi, G. Le Duc, S. Roux, P. Perriat, O. Tillement, *Angew. Chem. Int. Ed. Engl.* **2011**, *50*, 12299–12303.
[23] H. S. Choi, W. Liu, F. Liu, K. Nasr, P. Misra, M. G. Bawendi, J. V. Frangioni, *Nat. Nanotechnol.* **2010**, *5*, 42–47.
[24] Y. Matsumura, H. Maeda, *Cancer Res.* **1986**, *46*, 6387–6392.
[25] J. Morlieras, S. Dufort, L. Sancey, C. Truillet, A. Mignot, F. Rossetti, M. Dentamaro, S. Laurent, L. Vander Elst, R. N. Muller, R. Antoine, P. Dugourd, S. Roux, P. Perriat, F. Lux, J. L. Coll, O. Tillement, *Bioconjug. Chem.* **2013**, *24*, 1584–1597.
[26] P. Mowat, A. Mignot, W. Rima, F. Lux, O. Tillement, C. Roulin, M. Dutreix, D. Bechet, S. Huger, L. Humbert, M. Barberi-Heyob, M. T. Aloy, E. Armandy, C. Rodriguez-Lafrasse, G. Le Duc, S. Roux, P. Perriat, *J. Nanosci. Nanotechnol.* **2011**, *11*, 7833–7839.
[27] A. Bianchi, S. Dufort, F. Lux, A. Courtois, O. Tillement, J. L. Coll, Y. Cremillieux, *MAGMA* **2013**, *27*, 303–316.
[28] A. Mignot, C. Truillet, F. Lux, L. Sancey, C. Louis, F. Denat, F. Boschetti, L. Bocher, A. Gloter, O. Stephan, R. Antoine, P. Dugourd, D. Luneau, G. Novitchi, L. C. Figueiredo, P. C. de Morais, L. Bonneviot, B. Albela, F. Ribot, L. Van Lokeren, I. Dechamps-Olivier, F. Chuburu, G. Lemercier, C. Villiers, P. N. Marche, G. Le Duc, S. Roux, O. Tillement, P. Perriat, *Chemistry* **2013**, *19*, 6122–6136.
[29] T. H. Kuo, T. Kubota, M. Watanabe, T. Furukawa, S. Kase, H. Tanino, Y. Saikawa, K. Ishibiki, M. Kitajima, R. M. Hoffman, *Anticancer Res.* **1993**, *13*, 627–630.
[30] R. A. Madero-Visbal, J. F. Colon, I. C. Hernandez, A. Limaye, J. Smith, C. M. Lee, P. A. Arlen, L. Herrera, C. H. Baker, *Surg. Oncol.* **2012**, *21*, 23–29.
[31] C. T. Badea, K. K. Athreya, G. Espinosa, D. Clark, A. P. Ghafoori, Y. Li, D. G. Kirsch, G. A. Johnson, A. Annapragada, K. B. Ghaghada, *PLoS One* **2012**, *7*, e34496.
[32] R. P. Nishanth, R. G. Jyotsna, J. J. Schlager, S. M. Hussain, P. Reddanna, *Nanotoxicology* **2011**, *5*, 502–516.
[33] I. Pujalte, I. Passagne, B. Brouillaud, M. Treguer, E. Durand, C. Ohayon-Courtes, B. L'Azou, *Part. Fibre Toxicol.* **2011**, *8*, 10.
[34] S. G. Han, B. Newsome, B. Hennig, *Toxicology* **2013**, *306*, 1–8.
[35] I. T. Shevchenko, G. E. Resnik, *Neoplasma* **1968**, *15*, 419–426.
[36] W. S. Cho, R. Duffin, C. A. Poland, A. Duschl, G. J. Oostingh, W. Macnee, M. Bradley, I. L. Megson, K. Donaldson, *Nanotoxicology* **2012**, *6*, 22–35.
[37] S. Hadina, C. L. Wohlford-Lenane, P. S. Thorne, *Toxicology* **2012**, *291*, 133–138.
[38] K. E. Driscoll, D. L. Costa, G. Hatch, R. Henderson, G. Oberdorster, H. Salem, R. B. Schlesinger, *Toxicol. Sci.* **2000**, *55*, 24–35.
[39] D. L. Costa, J. R. Lehmann, D. Winsett, J. Richards, A. D. Ledbetter, K. L. Dreher, *Toxicol. Sci.* **2006**, *91*, 237–246.
[40] S. A. Shoyele, S. Cawthorne, *Adv. Drug. Deliv. Rev.* **2006**, *58*, 1009–1029.
[41] A. Bianchi, S. Dufort, F. Lux, P. Y. Fortin, N. Tassali, O. Tillement, J. L. Coll, Y. Cremillieux. *Proc. Natl. Acad. Sci USA* **2014**, *111*, 9247–9252.
[42] M. Keramidas, V. Josserand, C. A. Righini, C. Wenk, C. Faure, J. L. Coll, *Br. J. Surg.* **2010**, *97*, 737–743.
[43] M. Keramidas, F. de Fraipont, A. Karageorgis, A. Moisan, V. Persoons, M. J. Richard, J. L. Coll, C. Rome, *Stem Cell Res. Ther.* **2013**, *4*, 41.
[44] M. Morille, C. Passirani, S. Dufort, G. Bastiat, B. Pitard, J. L. Coll, J. P. Benoit, *Biomaterials* **2011**, *32*, 2327–2333.

Received: May 10, 2014
Revised: July 14, 2014
Published online: